Monte Carlo simulation of charge transport in amorphous GST

Enrico Piccinini[(*)], Fabrizio Buscemi[(*)], Thierry Tsafack[(*)],
Rossella Brunetti[(+)], Massimo Rudan[(*)], and Carlo Jacoboni[(+)]

[(*)]"E. De Castro" Advanced Research Center on Electronic Systems and
Department of Electronics, Computer Science, and Systems, University of Bologna
Viale Risorgimento 2, I-40136 Bologna, Italy
enrico.piccinini@unimore.it

[(+)]Physics Department, University of Modena and Reggio Emilia, and
CNR-INFM National Center on nanoStructures and bioSystems at Surfaces (S3)
Via Campi 213/A, I-41100 Modena, Italy

ABSTRACT

A microscopic particle description of the charge transport process in amorphous GST (a-GST) is presented in this paper, based on the assumption that electrical conduction in the amorphous phase is controlled by defects and trapped carriers. The physical model has been implemented in a Monte Carlo simulation coupled to the Poisson equation for a simple device formed by a nanometric layer of amorphous GST in contact with two planar metallic electrodes. The purpose of our research is to understand how and to which extent different aspects of the microscopic picture influence the electrical properties of the device when external tunable parameters, like operating current and temperature, are varied. Moreover the role of other parameters, often almost unknown in real devices like, e.g., trap energy levels and concentration, trap spatial distribution, is analyzed through focused simulated experiments with the purpose of pursuing a theoretical control of the threshold behavior so important for technological exploitation. Results obtained so far are compared with experiments, analytical models available in the literature, and the outcome of deterministic equations formulated by the authors for the system under investigation.

Key words: chalcogenides, GST, charge transport, Monte Carlo simulation, non-volatile memories

1. INTRODUCTION

Charge transport properties of the GST (i.e., $Ge_2Sb_2Te_5$) material, suitably-modeled for describing phase-change memory devices, are presently the main focus of a number of research activities in view of the application of this material in nonvolatile-memory technology [1–3]. Experimental structural data and charge-transport features of GST-based devices suggest that electrical conduction in the amorphous phase is controlled by defects and trapped carriers [4,5]. Recent *ab initio* studies of the atomic structure and the electronic and optical properties of a-GST [6] provided further insight into the origin of these defects/traps. This was accomplished by an analysis of the atomic structure of a-GST and of the modification of the coordination number of Ge, Sb and Te, with respect to the cubic phase, when GST is quenched from the melt. Ielmini and Zhang [5] provided a good interpretation of the $I(V)$ characteristics obtained for an a-GST film between two electrodes by means of an analytical 1D model for the trap-limited conduction. In the below-threshold regime they assume that the transfer of an electron between traps and from/to traps to/from contacts occurs via thermal emission over the potential barrier (TE) at donor-like traps, described by the Pool-Frenkel model suitably modified in order to account for the effect of the charge trapped in the device on the potential barrier. Tunneling through the potential barrier separating two traps is accounted for as a TE component, affecting the amplitude and the dependence of the current on temperature, but not its functional form [7]. In the above-threshold regime the theory of [5] adds to the TE effect also the field-assisted tunneling and the spatial non-uniformity of the electric field, which are interpreted as the main effects responsible for the snap-back behavior of the $I(V)$ curve.
The aim of our work is to formulate a theoretical framework for charge transport in a-GST based on a hopping conduction picture, and to apply it in a Monte Carlo simulation of a simple device in order to understand how and to

what extent different aspects of the microscopic picture influence the electrical properties of the device when external tunable parameters, like operating current and temperature, are varied. Moreover the role of other parameters, often almost unknown in real devices like, e.g., trap energy levels and concentration, and trap spatial distribution, is analyzed through focused simulated experiments, with the purpose of pursuing a theoretical control of the threshold behavior, very important for technological exploitations. Section 2 is dedicated to the illustration of the physical model and the theoretical approach. Section 3 illustrates the details of the Monte Carlo simulation scheme and the results obtained so far from the simulations. The rate kinetic equations used as "simple&quick" probe of the transport model are described in section 4. Section 5 collects the main conclusions of our work so far. Since the model is still under development, further refinements in the physical models and improvements in the simulation tools are planned for the near future.

2. THE PHYSICAL MODEL

In the trap-conduction model we used to describe electron transport in a-GST, the current flow is due to electron hopping among donor-type traps. The present numerical implementation includes two donor levels (type-I and type-II traps), located 0.01 eV below and 0.29 eV above the Fermi level of the system. In order to guarantee the electrical neutrality, a number of acceptor levels, not involved in the transport process, is assumed in order to ensure material compensation. Following the variable-range hopping theory [8], electrons are thought to tunnel from one centre to the next. The transition rate S_{ij} for electron hopping from occupied site i to empty site j is evaluated according to [9]:

$$\begin{aligned} S_{ij} &= \nu_0 e^{-2\alpha R} e^{-\frac{\varepsilon_j - \varepsilon_i + e\varphi_j - e\varphi_i}{kT}} \quad \text{if} \quad \varepsilon_j - \varepsilon_i + e\varphi_j - e\varphi_i > 0 \\ S_{ij} &= \nu_0 e^{-2\alpha R} \quad \text{if} \quad \varepsilon_j - \varepsilon_i + e\varphi_j - e\varphi_i \le 0 \end{aligned} \tag{1}$$

where ν_0 is the attempt-to-escape frequency, R is the distance between the two trap sites, α is a factor depending on the overlap of the wave functions and, therefore, on the energy-barrier height between the sites, ε_i is the energy level of the trap, and φ_i the electric potential in the ith site. The potential φ_i is determined by both the external bias and the trap charges. In this early stage of development of our theory, phonon-assisted tunneling, thermal jumps over the barrier, and transitions to the conduction-band states have not been included.

3. MONTE CARLO SIMULATION SCHEME AND RESULTS

The model described in the previous section has been implemented into a 3D Monte Carlo simulation of the electron motion in an a-GST sample (size: 30×30×30 nm^3) in contact with two planar metallic electrodes. A number N of each type of traps described above are positioned at random inside the sample. All relevant transitions between traps and from traps (contacts) to contacts (traps) are accounted for. Eq. (1) has also been used to calculate the transition rate from trap to contact and from contact to trap, taking R as the closest distance between the trap and the involved contact.

The simulation is current driven, consistently with the typical experimental setup. This is achieved by adding (subtracting) an electron to the left (right) contact every Δt, with $\Delta t = e/I$ (e and I being respectively the electron charge and the current intensity).

The potentials φ_i and φ_j involved in the transition rates from trap i to trap j, Eq. (1), are determined by the contribution of the charged contacts, of all of the unoccupied donor traps except trap j, and by the compensating charges. It is worthwhile understanding how crucial the description of the electrostatics for reaching a stationary condition is, and, from a different viewpoint, also for the device operation itself.

The self-consistent electrostatics has been dealt with in two different ways either by solving the Poisson equation with the finite-element method or by evaluating the potential at each point of interest as the direct sum of the contributions of all the present charges. Due to the high computational load required to self-consistently solve the Poisson equation in a 3D environment in the transport framework, the second method, though more simplified, was mainly used at this stage thanks to its faster implementation. The system showed a high sensitivity to the way electrostatics had been accounted for, but the two approaches yielded comparable results under similar conditions.

The scheme outlined above has been applied to the simple device described at the beginning of this section, for a number of different trap concentrations, all comparable with experimental conditions. In Fig. 1 three $I(V)$ curves are reported for 50, 100, and 150 traps per type. The results have been obtained at room temperature with $\nu_0 = 10^{12}$ s^{-1}.

The dependence of α in Eq. (1) on the energy-barrier height has been modeled through the following formula [10] under the simplifying hypothesis of a rectangular barrier:

$$\alpha^2 = \alpha_0^2 - \frac{m_0 e}{\hbar^2}\left|\varphi_i - \varphi_j\right| \tag{2}$$

where $\alpha_0 = 0.2$ nm^{-1} and m_0 can be viewed as an averaged electron effective mass.
The voltage values in the three curves of Fig. 1 have been obtained as averages of the final voltage over 25 independent simulations, each of them lasting 1 ns. This time proved to be enough to reach the steady-state value. The data showed a strong dependence on the random geometrical distribution of the traps, justified by the small number of traps inside the nanometric-size device.

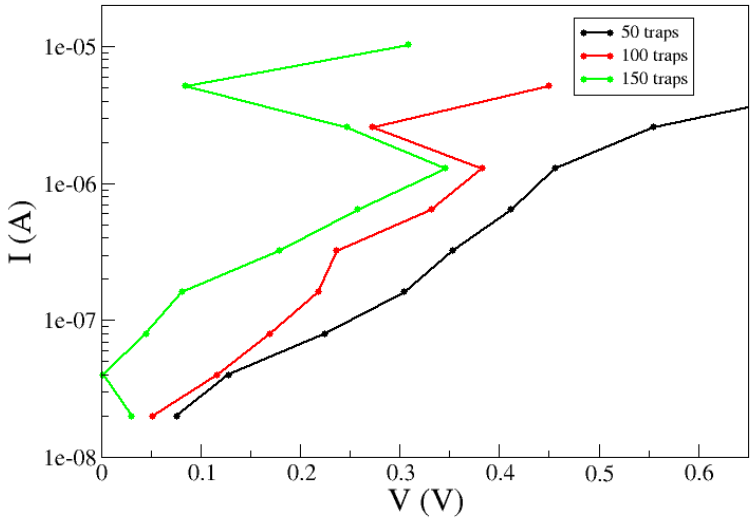

Figure 1 — *I*(*V*) curves obtained with the MC simulation model, with a different number of traps per type included in the simulations as indicated in the box. Voltage results have been averaged over 25 runs; the standard deviation affecting each point is about 0.05, 0.08 and 0.1 V for 50, 100 and 150 traps, respectively.

The overall shape of the curves is in qualitative agreement with both experiments and previously-developed analytical models. In particular we stress that the current at which the snap-back effect takes place is almost constant (about 1μA), consistently with experiments. It is also worthwhile noting that if the number of traps included in the simulation is too low, the snap-back effect is not revealed by the calculations.
The Monte Carlo simulation allows one to explore microscopic features of the system which provide a deeper understanding of the snap-back onset. Fig. 2 illustrates the spatial charge distribution (top), the electric field component (middle), and the potential profile (bottom) along a direction perpendicular to the contacts for current values lower than, equal to, and higher than the reported threshold value for the case of 100 traps per type. We point out that as the snap-back effect occurs, the device is subdivided into two well defined domains with opposite charges, which produce a non-monotonic behavior of the electric field and, in turn, a maximum of the potential profile inside the device. This situation is quite different from the one reported before the snap-back effect, where the charge is almost uniformly distributed along the device, and the electric field and its associated potential are monotonically-increasing functions of the spatial coordinate.
A better insight of this effect is provided by Fig. 3, where the total charge has been split into its three components linked to the three different types of traps. The red curves describe the type-I traps, which below threshold are mostly filled, while the green curves show the type-II traps, which below threshold are mostly empty. As the injected current increases a charge redistribution occurs, such that the type-I traps are completely filled near the right contact, whereas the fraction of filled traps decreases near the left contact. The type-II traps exhibit a similar behavior, however, the fraction of empty traps near the left contact is substantially larger for the type-II traps than for the type-I traps. As both

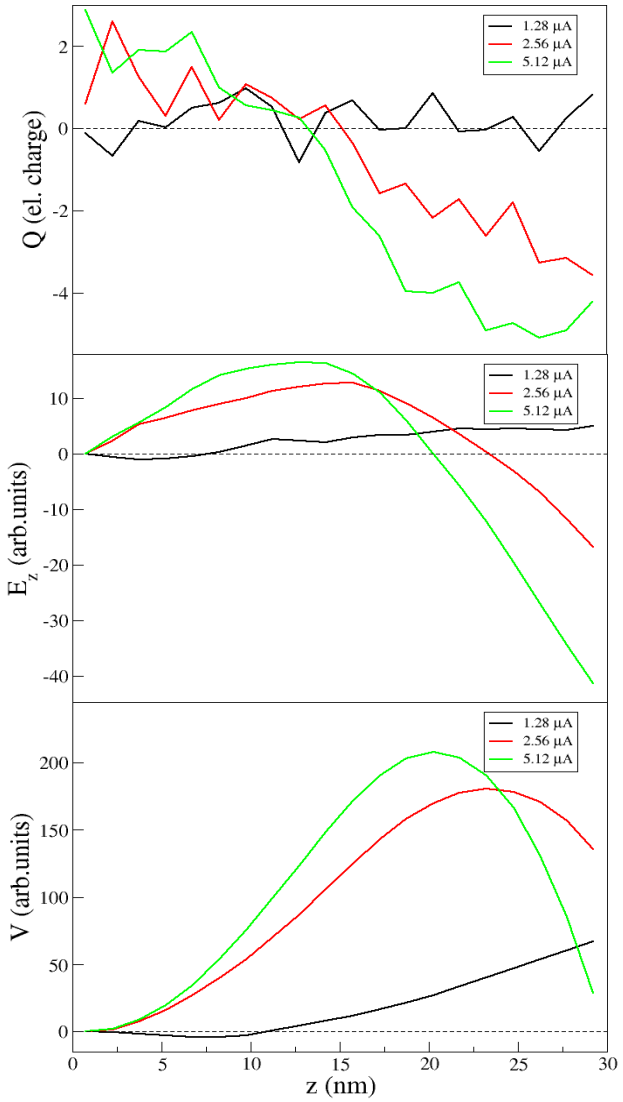

Figure 2 — Total space charge distribution (top), electric field (middle) and potential profiles (bottom) along the device for the three currents indicated in the boxes, using 100 traps per type. The total charge is obtained by performing first 25 independent Monte Carlo simulations, then averaging their results within each of the 1.5 nm-wide bins, parallel to the contacts, into which the device is subdivided. The electric field and the potential have been calculated by successive integrations.

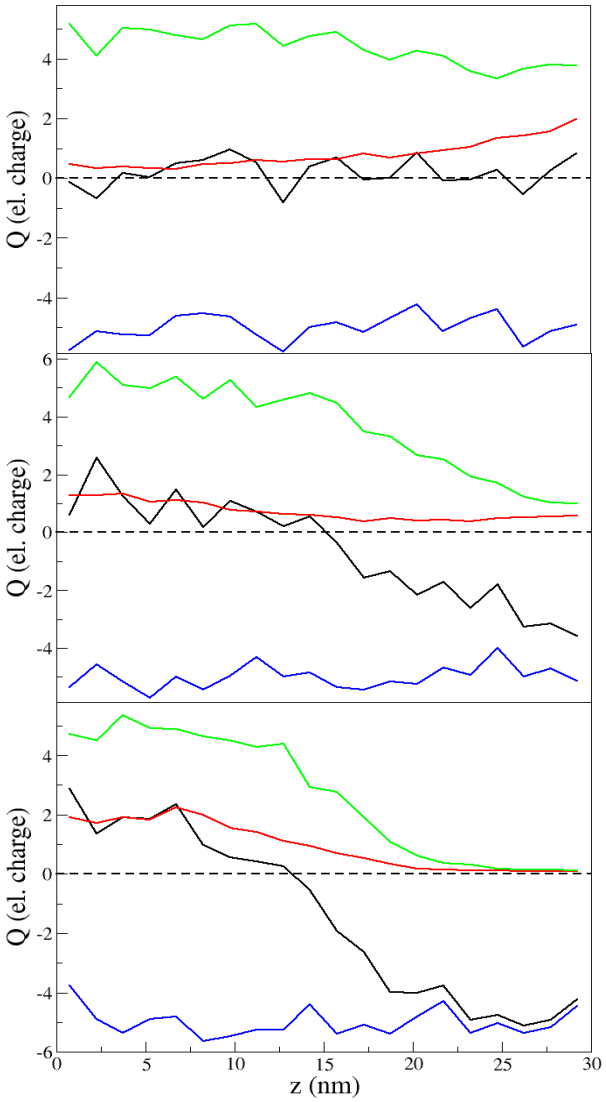

Figure 3 — Space charge profile along the device for the three currents 1.28 µA (top), 2.56 µA (middle) and 5.12 µA (bottom). The black, red, green and blue lines stand for the total charge, the contribution to the total charge due to type-I traps, the contribution due to type-II traps, and to the compensating charge, respectively. Data are collected as explained in Fig. 2.

type-I and type-II traps are neutral when filled, the compensating charge (blue curves) makes the net charge (black curves) increasingly negative on the right half of the device, and positive on the left side. This better explains the behavior of the curves of Fig. 2 (top).

4. RATE KINETIC EQUATIONS FOR A TRAP-LIMITED TRANSPORT MODEL

In parallel with the Monte Carlo approach, a deterministic model based on rate equations for the traps has been devised. To make the model readily consistent with the solution of the Poisson equation, the rate equations are based on the concept of box. In each box different types of traps are present, each type being characterized by the position of the ground state with respect to the Fermi level at equilibrium and by the energy values of the excited states. The electrons stored in the traps belonging to the *i*th box give rise to the charge density of the box. If the traps of the *i*th box exchange electrons among each other, the charge density of the box is not influenced, however, these exchanges influence the dynamics of the electrons and must be accounted for anyhow.

It is assumed that, for each type of traps, two energy levels at most are involved in the exchanges, labeled E_a and E_b, with $E_b > E_a$. When both levels are filled, the trap is negatively charged. When both are empty, the trap is positively charged. Finally, the trap is neutral when one level is filled and the other is empty. In this case it is also assumed that the filled level is E_a. With these assumptions, an electron may be emitted by a trap only when the latter is negative or neutral, whereas an electron may be captured by a trap only when the latter is neutral or positive. In conclusion, depending on the charge content of the traps, four electron-exchange processes may take place: from a negative trap to a neutral or a positive one, and from a neutral trap to a neutral or positive one.

The probability per unit time of an electron transition from a trap at position $\boldsymbol{r}'$ to a trap at position $\boldsymbol{r}''$ depends on the charge content if each trap, their distance, and the energy difference between the initial and final level. Such a difference, in turn, depends on the type of the two traps and on the distribution of charge within the device. As a consequence, the transition probability per unit time is not symmetrical upon exchange between the two traps. Another possible exchange process is the electron transition between a trap and one of the contacts. As the latter are treated as reservoirs, they are in any case able to receive electrons from negative or neutral traps, and to give electrons to positive or neutral traps. Another remark is that the contacts are spatially extended, whereas the traps are point-like. As a consequence, one may assume that the distance that influences the transition is the minimum distance between the contact and the trap. Direct transitions from one contact to the other are not considered because their probability is negligible.

To simplify the notation, only one type of traps will be considered in this section. The same analysis must be repeated for all types of traps. Let N_i , N_j be the concentrations of traps of the chosen type belonging to the *i*th and *j*th box, respectively. The indices play the role of spatial coordinates, hence they replace the coordinates $\boldsymbol{r}'$ and $\boldsymbol{r}''$ used before. The probabilities per unit time of the four possible electron-exchange processes between the traps are indicated with S_{ij}^{-0}, S_{ij}^{-+}, S_{ij}^{00}, S_{ij}^{0+}, where the left (right) apex indicates the state of charge of the trap emitting (capturing) the electron prior to the transition. The expressions of the probabilities per unit time have the form given in Eq. (1). Similarly, the probabilities per unit time of the exchange processes between traps of the *i*th box and the left contact are indicated with S_{iL}^{-}, S_{iL}^{0}, S_{Li}^{0}, S_{Li}^{+} (replacing L with R provides the symbols for the transitions to/from the right contact). The concentration N_i is the sum of the concentrations of positive, negative, and neutral traps of the chosen type belonging to the *i*th box. It is useful to introduce the fractions α_i^+, α_i^-, α_i^0, ranging from 0 to 1, such that the concentration of positive traps is $N_i\alpha_i^+$, and so forth. As a consequence, the chosen type of traps contributes to the charge density of the *i*th box as $\rho_i = eN_i\,(\alpha_i^+ - \alpha_i^-)$, with e the electron charge. In each box the fractions vary with time, however they must fulfill the relation $\alpha_i^+(t) + \alpha_i^-(t) + \alpha_i^0(t) = 1$, so actually only two fractions are independent. In the following, α_i^+ and α_i^- will be considered. The fractions, as long as the trap concentration N_i , vary also in space. This eventually yields a charge density that varies in space and time. For the chosen type, the number of positive (negative) traps of the *i*th box is $\Omega_i N_i \alpha_i^+$ ($\Omega_i N_i \alpha_i^-$), where Ω_i is the volume the box.

The rate equations are written in terms of the fractions α_i^+ and α_i^- of each box. More precisely, they express the time variation $\Omega_i N_i\, \mathrm{d}\alpha_i^+/\mathrm{d}t$ as the sum of the electron transitions per unit time that increase α_i^+, less the sum of the transitions that decrease it. The same holds for $\Omega_i N_i\, \mathrm{d}\alpha_i^-/\mathrm{d}t$. This provides a set of $2M_B$ equations in the $2M_B$ unknowns α_i^+ and α_i^-, $i = 1,2,\ldots, M_B$. Here M_B is the number of boxes belonging to nodes internal to the device or lying along the insulating boundaries. The equations are obviously non linear, because the product of the fraction of electron-emitting traps times the fraction of electron-capturing traps appears in each summand. To complete the set of rate equations it is necessary to add two more equations, that express the time variations of the number of electrons in the left and right contacts. They have the same structure as those associated to the boxes, the only difference being that it is necessary here to add the contribution of the current generator connected to the contacts. If I is the current

injected by the generator, such a contribution has the form, say, $-I/q$ for the left contact and I/q for the right one. In total, there are $M_B + 2$ rate equations in $M_B + 2$ unknowns.

The rate equations contain also the probabilities per unit time defined in (1). For a given pair ij of box indices, each probability per unit time depends on the difference $\varphi_i - \varphi_j$, where φ is the electric potential. It is therefore implied that in the solution of the rate equations the electric potential is preliminarily known. This is in fact not true, because the electric potential depends on the number of trapped charges, so it is also an unknown. The model is then completed by adding the Poisson equation and solving it self-consistently with the rate equations.

It is interesting to note that the formal structure of the rate equations is similar to that of a standard Boltzmann transport equation, namely, "*total time variation = scattering-in – scattering-out*". The equations contain the indices of the cells of the phase space. Those related to the coordinate space are the box indices, i, j. Those of the momentum space are the apices "–","0", and "+". In principle, the momentum space should contain all the indices counting the energy eigenvalues of the traps. However, as the energy values are all that matters in this context, the number of indices is reduced by summing over the indices related to the angular variables and over the spin index, this leaving a single index. The number of values of the latter is further reduced by considering only the two energies E_a and E_b, as indicated above. Despite the formal analogy with the Boltzmann transport equation, there are important differences between the latter and the rate equations of the model presented here. In the collision term of the Boltzmann equation, at least in the form commonly used to model solid-state devices, the momentum space is used in its entirety, while the coordinate space is eliminated because it is assumed that the transitions due to collisions take place without an appreciable displacement of the electron in the coordinate space. In contrast, in the rate equations of the present model the momentum space is strongly reduced, whereas the real space is used in its entirety. These differences impose a rather non-standard implementation of the numerical-solution schemes, including those of the Monte Carlo code described in section 3.

A significant aspect of the rate equations is that a simplified form of theirs lends itself to an analytical solution. The latter shows that the parameter controlling the departure of the device from equilibrium is proportional to the ratio I/ν_0. This is sensible from the physical standpoint, since an increasing attempt-to-escape frequency ν_0 balances the effect of the driving signal I.

5. CONCLUSIONS AND PERSPECTIVES

An approach to the transport problem in amorphous GST materials, based on the assumption that the electrical conduction in the amorphous phase is controlled by defects and trapped carriers, has been shown in this paper. The physical model differs from those used so far in the literature for the analysis of phase-change memories. The preliminary results are encouraging and stimulate further refinements of the theory. In this respect, several aspects may be tackled. For instance, at present only two trap levels are included in the Monte Carlo scheme: future developments of the model will include trap bands as well as transitions from localized to extended conduction-band states.

Another aspect is the electrostatic part of the simulations, whose important role has been anticipated in section 3. The fully 3D, self-consistent solution of the Poisson equation coupled with the Monte Carlo simulation is very demanding. Nevertheless, in the Monte Carlo simulations presented here the electron transitions between two traps have in fact been treated by considering two point-like Coulombic centers in three dimensions. In contrast, to speed up the calculations, in the transition between a contact and a trap the charge of the latter has preliminarily been spread over a plane parallel to the contact. This has been done to the purpose of keeping the electric potential constant over the contact without resorting to the image-charge method: the latter, in fact, would significantly alter the total charge due to the small number of charges trapped inside the device. Spreading the trapped charge over a plane is equivalent to treating the interaction between a trap and a contact as a 1D problem. Finally, another issue that needs to be improved is the contribution of the barrier lowering to the parameter α in (2), whose expression, as mentioned in section 3, is derived from the standard expression of tunneling through a rectangular barrier.

This work has been carried out under the contract 34524/2007 of the Intel Corporation, whose support is gratefully acknowledged.

REFERENCES

1. Kim *et al.*, Proc. ISSCC 2004, 662 (2004).

2. S. Lai, Tech. Digest, Int. Electron Devices Meeting (IEDM) 2001, 803 (2001).

3. S. Lai, Tech. Digest, Int. Electron Devices Meeting (IEDM) 2003, 255 (2003).

4. C. B. Thomas, J. Phys. D **9**, 2587 (1976).

5. D. Ielmini *et al.*, J. Appl. Phys. **102**, 054517 (2007).

6. S. Caravati *et al.*, Appl. Phys. Lett. 91, 171906 (2008).

7. D. Ielmini and Y. Zhang, Tech. Digest, Int. Electron Devices Meeting (IEDM) 2006, 401 (2006).

8. N. F. Mott and E. A. Davis, "Electronic Processes in Noncrystalline materials", Clarendon Press, Oxford (1961).

9. A. Miller and E. Abrahams, Phys. Rev. **120,** 745 (1960).

10. E. Merzbacher, "Quantum Mechanics", John Wiley & Sons, New York (1961).

AUTHORS' BIOGRAPHIES

Enrico Piccinini received the *Laurea cum laude* in Materials Engineering at the University of Modena and Reggio Emilia, Italy, in 2000, and the PhD in Chemical, Environmental Engineering and Safety at the University of Bologna, Italy, in 2004. Since 2004 he has been working with the Department of Electronics, Computer Science and Systems of the University of Bologna under a research contract. His research interests include the analysis of combined effects of dilation and mass transport in polymeric systems, numerical modelling of non-Fickian diffusion, the design and testing of prototype apparatuses for the simultaneous measurement of mass sorption, diffusion and dilation in polymeric films, theoretical and computational modelling of charge-transport properties in ion channels and newly-designed semiconductor materials by means of Molecular Dynamics and Monte Carlo simulation techniques.

Fabrizio Buscemi received the *Laurea cum laude* in Physics in 2004 at the University of Palermo, Italy, and the PhD in Physics at the University of Modena and Reggio Emilia, Italy, in 2007. Since January 2008 he has been working under a research contract at the ARCES Research Center of the University of Bologna, Italy. His research interests include theoretical and computational analysis of entanglement dynamics for charges interacting in semiconductor nanostructures and Monte Carlo simulations of charge transport in semiconductor structures and devices.

Thierry Tsafack completed his high-school studies in Cameroon and graduated in electrical engineering at the University of Bologna in 2006. He is at present graduate student in the PhD Program in Electrical Engineering of the University of Bologna. His research interests include electron transport and scattering mechanisms within cylindrical nanowire MOSFET devices, and the investigation of electronic and transport properties of the phase-change material $Ge_2Sb_2Te_5$ for data storage applications.

Rossella Brunetti received the *Laurea cum laude* in Physics in 1981 and the PhD in Physics at the University of Modena, Italy, in 1987. She has been working at the Physics Department of the University of Modena and Reggio Emilia, Italy, as teaching and research assistant since 1990. From 2002 she is associate professor in Physics at the Physics Department and the Pharmacy Faculty of the same University. Past and present research interests include: theory of electron transport in semiconductors in semiclassical and quantum conditions, numerical-simulation techniques (mainly the Monte Carlo and Molecular Dynamics approaches) applied to the analysis of semiconductor

structures and devices, quantum transport problems in mesoscopic structures and low-dimensional systems, and, more recently, ion conduction across nanometric ion channels of the cell membrane.

Massimo Rudan received the degree in electrical engineering in 1973 and the degree in physics in 1976, both from the University of Bologna, Italy. He joined the Department of Electronics (DEIS), University of Bologna, in 1975. In 1990, he was appointed Full Professor of Microelectronics. Since 1983, he has been working in a group involved in the investigations of the physics of carrier transport and numerical analysis of semiconductor devices. In 1985 to 1986 he was a Visiting Scientist at the IBM Thomas J. Watson Research Center, Yorktown Heights, NY, studying the discretization techniques for the higher-order moments of the Boltzmann transport equation. His research interests are in the physical and numerical modeling of nanodevices and of solid-state sensors. M. R. is Fellow of IEEE.

Carlo Jacoboni obtained his PhD in Physics in 1969 at Purdue University, West Lafayette, Indiana (USA). He is full Professor of Atomic Physics at the University of Modena and Reggio Emilia. He has published several books and about 160 scientific papers in international journals in the field of charge transport in semiconductors. He has been Director of several national and international Schools and Conferences on Transport in Semiconductors and Principal investigator of national and international Research Contracts. His scientific activity has been related to electron transport in semiconductor materials and devices and to the theory of quantum transport in mesoscopic structures in coherent and dissipative regimes. He is Fellow of the American Physical Society.